

1 **Supplemental material for:**
2 **CPSF3 inhibition blocks pancreatic cancer cell proliferation**
3 **through disruption of core histone mRNA processing**
4

5 Abdulrahman. A. Alahmari, Aditi H. Chaubey, Venkata S. Jonnakuti, Arwen A. Tisdale,
6 Carla D. Schwarz, Abigail C. Cornwell, Kathryn E. Maraszek, Emily J. Paterson, Minsuh
7 Kim, Swati Venkat, Eduardo Cortes Gomez, Jianmin Wang, Katerina V. Gurova, Hari
8 Krishna Yalamanchili, and Michael E. Feigin*

9

10 *Corresponding author:

11 **Email:** michael.feigin@roswellpark.org

12

13

14 **This PDF file includes:**

15 Supplemental Figures S1 to S13

16 Supplemental Figure Legends S1 to S13

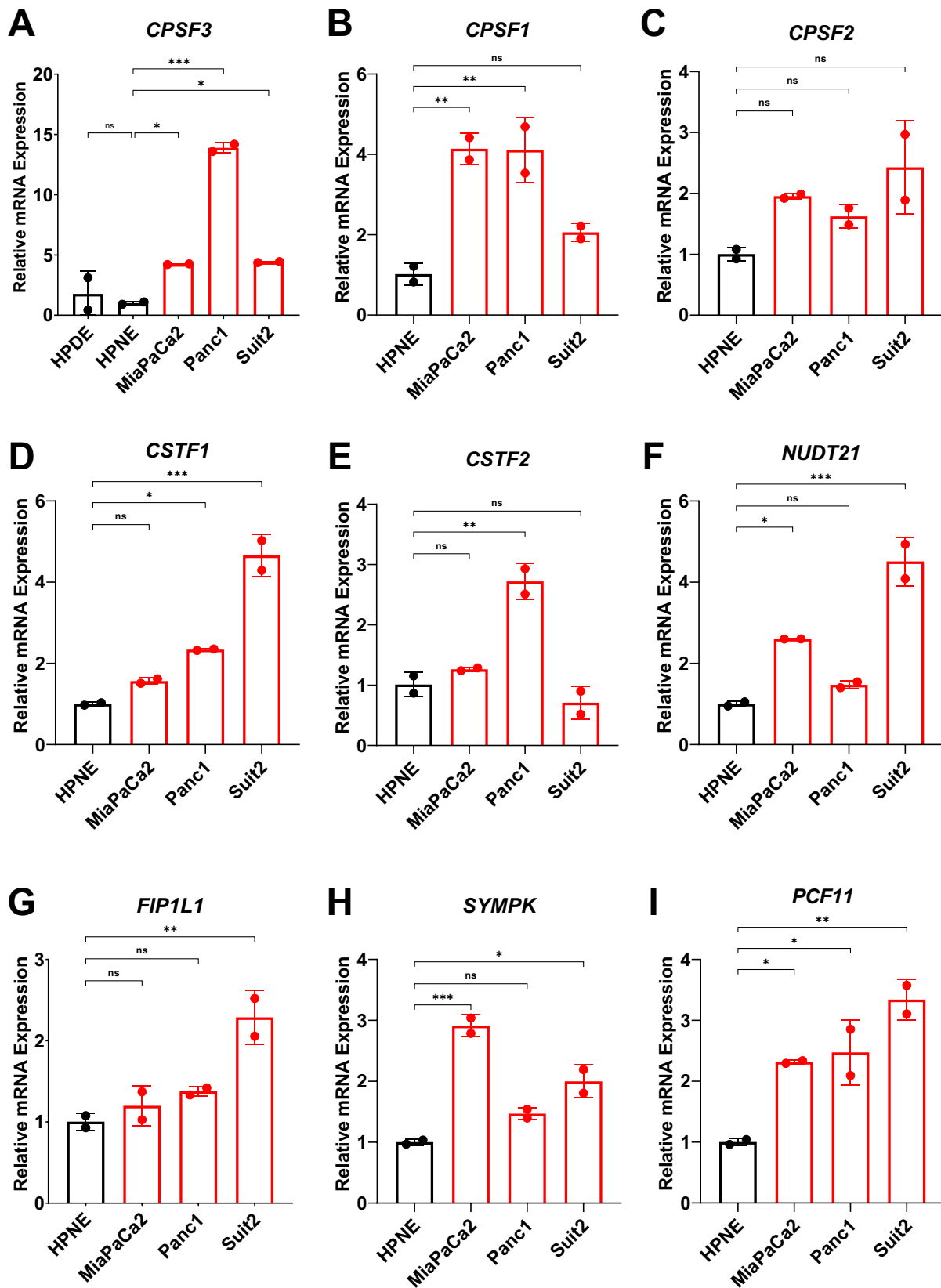
17 Materials and Methods

18 Tables S1

19 Tables S2

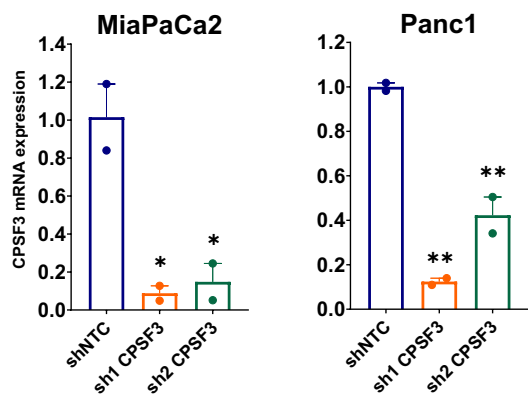
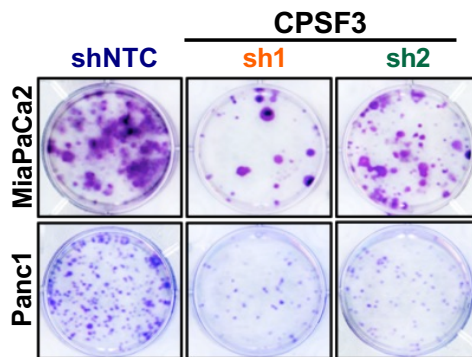
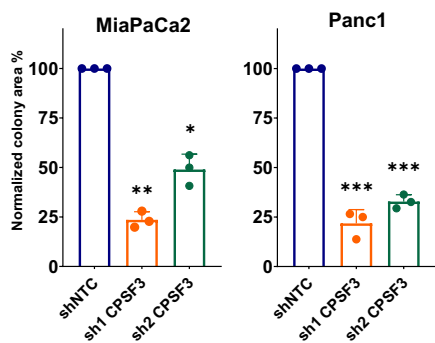
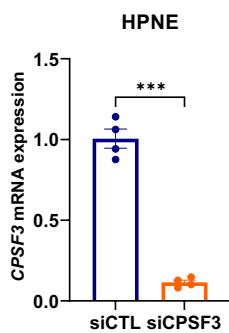
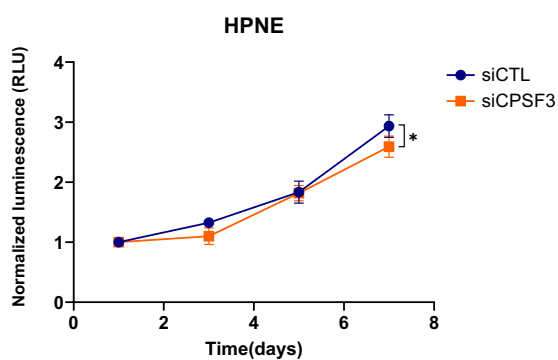
20 References

Supplemental Fig S1



21 **Fig. S1. Multiple CPA factors are upregulated in PDAC cells.**
22 **(A-I)** Quantitative RT-PCR showing mRNA expression levels of multiple CPA factors in
23 non-transformed pancreatic epithelial (black) and PDAC (red) cells. Data are shown as
24 mean \pm SD. *, $P < 0.05$; **, $P < 0.01$; ***, $P < 0.001$; Ordinary one-way ANOVA with
25 Dunnett's multiple comparisons test.
26
27

Supplemental Fig S2

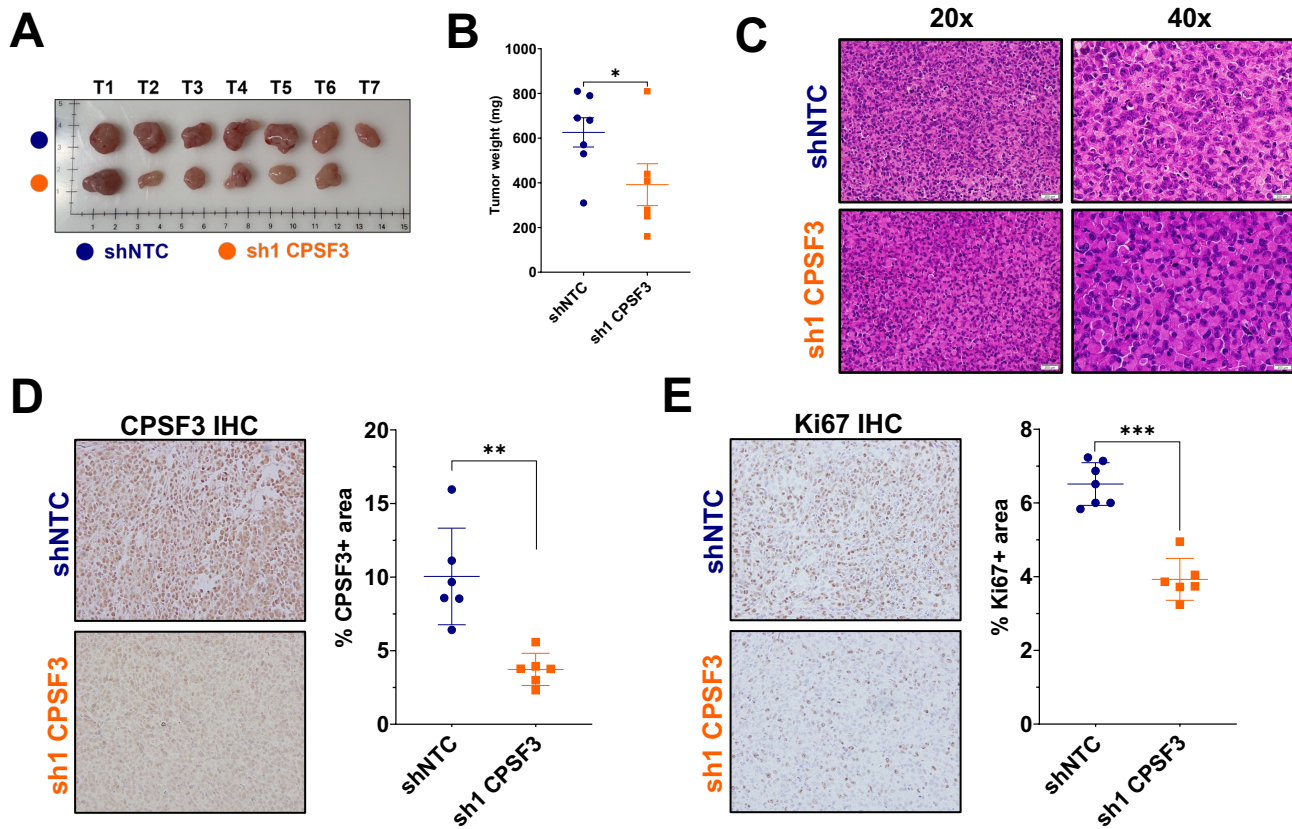
A**B****C****D****E**

28 **Fig. S2. PDAC cells, but not immortalized control cells, are affected by CPSF3**
29 **knockdown.**

30 **(A)** mRNA expression of *CPSF3* in shNTC, sh1 *CPSF3* and sh2 *CPSF3* knockdown cells
31 by qPCR. Graphs are representative of at least two independent experiments. Data are
32 shown as mean \pm SEM of technical duplicates. **, $P < 0.01$, Ordinary one-way ANOVA
33 with Dunnett's multiple comparisons test. **(B)** Clonogenic growth assay of shNTC (blue),
34 sh1 (orange) and sh2 (green) *CPSF3* knockdown cells. **(C)** Normalized colony area
35 percentage of shNTC, sh1 and sh2 *CPSF3* knockdown cells from **(B)**. *, $P < 0.05$; **, $P <$
36 0.01 ; ***, $P < 0.001$; Ordinary one-way ANOVA with Dunnett's multiple comparisons test.
37 **(D)** Quantitative RT-PCR showing *CPSF3* mRNA expression levels in HPNE cells upon
38 *CPSF3* transient knockdown by siRNA. Data are shown as mean \pm SEM. **, $P < 0.001$,
39 unpaired t test. **(E)** Proliferation rates at days 0, 2, 4 and 6 of immortalized control HPNE
40 cells upon *CPSF3* knockdown. Data are shown as mean \pm SD. *, $P < 0.05$; 2way ANOVA
41 with Sidak's multiple comparisons test.

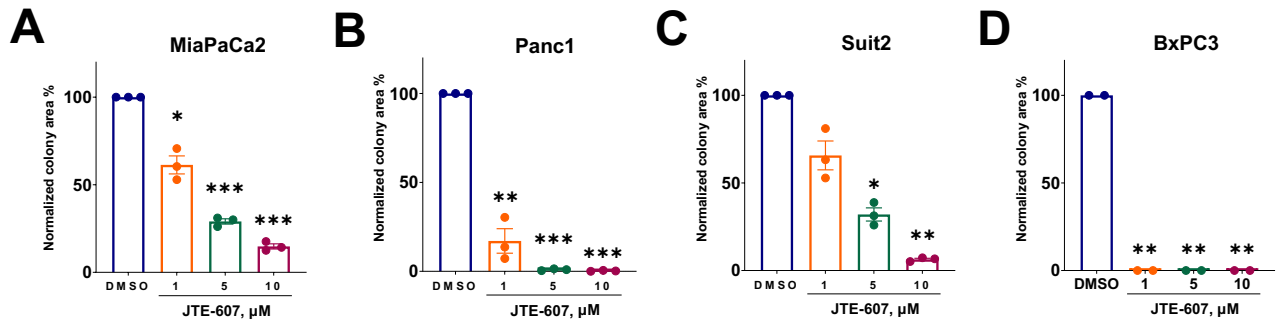
42
43

Supplemental Fig S3



44 **Fig. S3. CPSF3 knockdown decreases proliferation in vivo.**
45 **(A)** Gross images of shNTC (n=7, blue) and shCPSF3 (n=6, orange) dissected tumors.
46 **(B)** Endpoint tumor weight. *, $P < 0.05$, unpaired t test with Welch's correction. **(C)**
47 Hematoxylin and Eosin (H&E) staining of shNTC (left) and sh1 CPSF3 (right) xenograft
48 tumors (MiaPaCa2 cells). **(D, E)** Representative IHC for CPSF3 and Ki67, respectively.
49 Box and whisker plots indicate the percentage of CPSF3- and Ki67-positive areas in the
50 tumors. **, $P < 0.01$; ***, $P < 0.001$; unpaired t test.
51
52

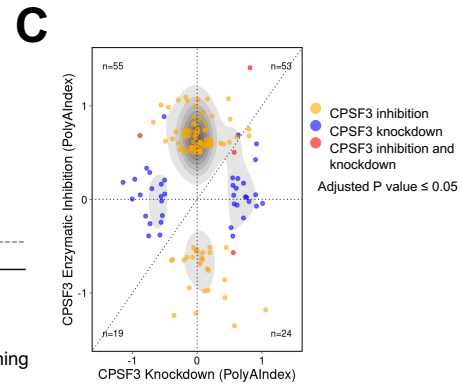
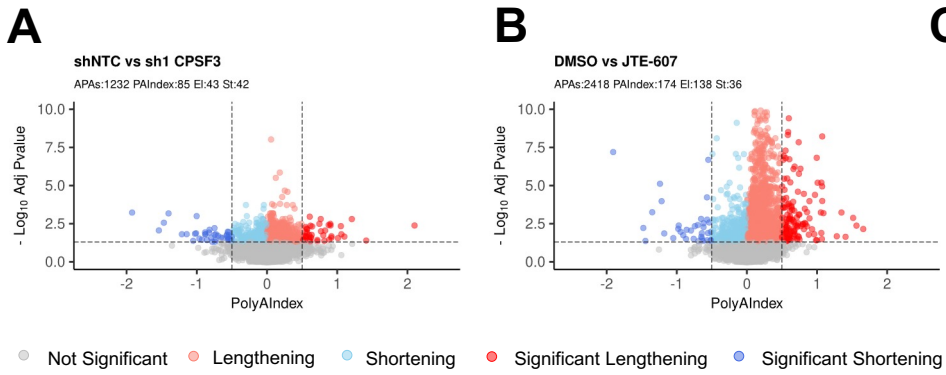
Supplemental Fig S4



53 **Fig. S4. JTE-607 decreases colony formation of PDAC cells.**
54 **(A-D)** Normalized colony area percentage of PDAC cell lines from **Figure 2F**. *, $P < 0.01$;
55 **, $P < 0.001$; ***, $P < 0.0001$; Ordinary one-way ANOVA with Dunnett's multiple
56 comparisons test. Data are shown as mean \pm SEM.

57
58

Supplemental Fig S5



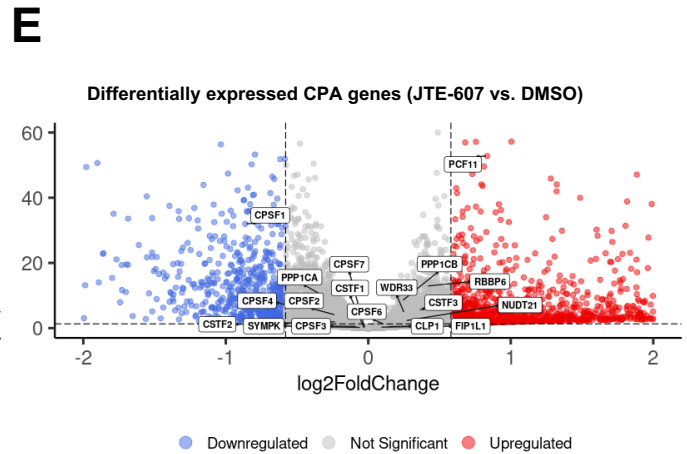
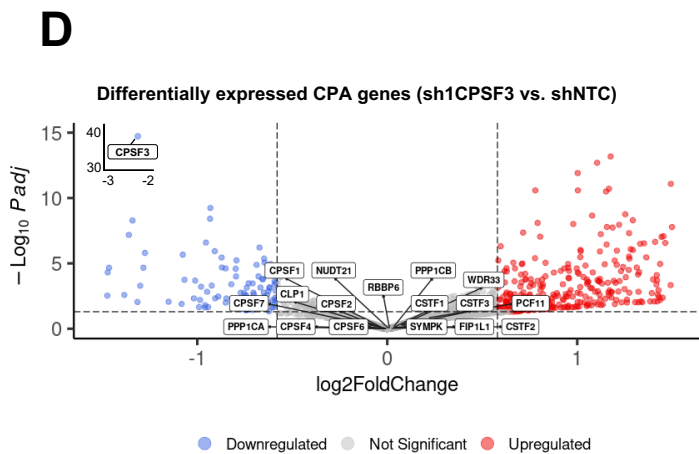
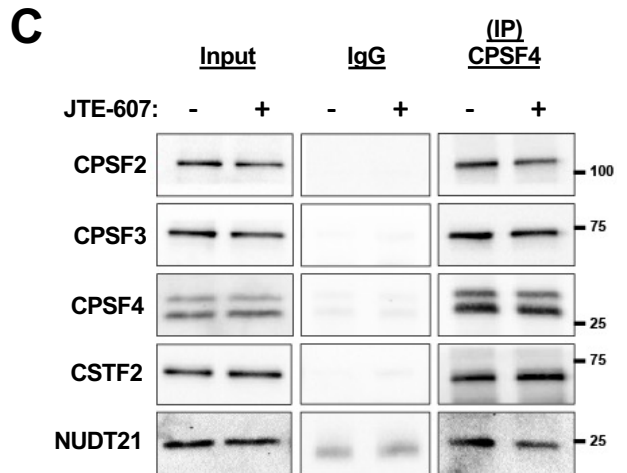
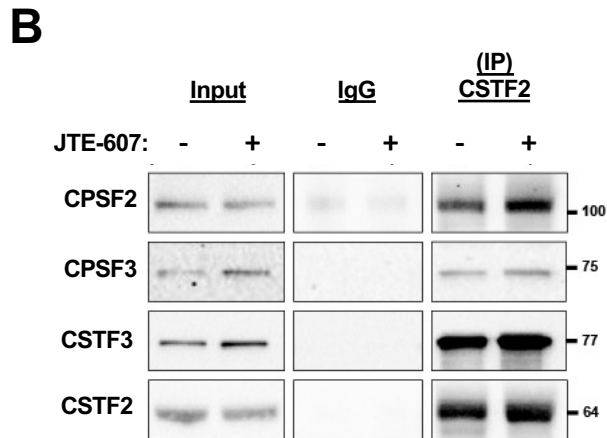
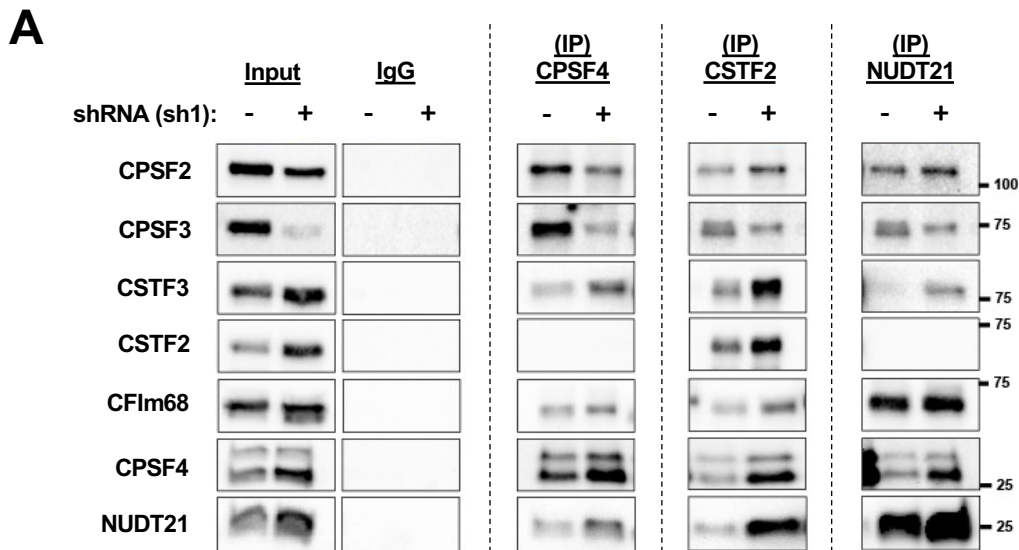
59 **Fig. S5. mRNA 3'-end processing is distinct between CPSF3 knockdown and**
60 **inhibition.**

61 **(A, B)** Volcano plots showing differential CPA genes ($-0.5 > \text{PolyAIndex} > 0.5$; $P < 0.05$).
62 Blue dots indicate 3'-UTR shortening while red dots indicate 3'-UTR lengthening.
63 Significant shortening genes = 42 and 36 upon *CPSF3* knockdown and inhibition,
64 respectively. Significant lengthening genes = 43 and 138 upon *CPSF3* knockdown and
65 inhibition, respectively. **(C)** Dot plot with quadrants representing APA differences in both
66 *CPSF3* knockdown (72hr post transduction) and inhibition (24hr post JTE-607 treatment).
67 Only 2 genes are uniquely altered in both conditions (Red dots, top-right quadrant); DAGs
68 = differential APA genes.

69

70

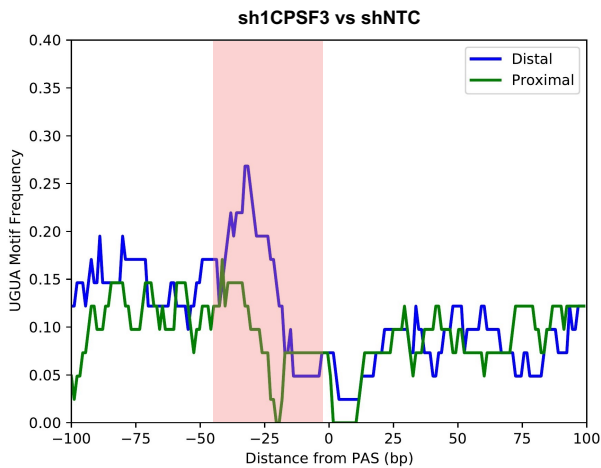
Supplemental Fig S6



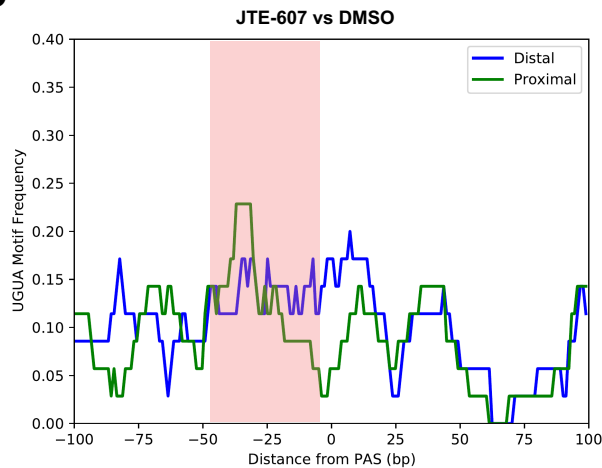
71 **Fig. S6. CPSF3 knockdown, but not inhibition, destabilizes the CPA complex.**
72 **(A – C)** Western blots of the immunoprecipitation (IP) assay using (left to right) anti-
73 CPSF4, anti-CSTF2 and anti-NUDT21 to co-immunoprecipitate different components of
74 the CPA complex. IP experiments were performed using *CPSF3* knockdown **(A)** and
75 JTE-607 treated cells **(B and C)**. **(D, E)** Volcano plots of differentially expressed genes
76 upon *CPSF3* knockdown and inhibition, respectively. Blue and Red dots indicate
77 downregulated and upregulated genes, respectively (FC>1.5, Adjusted *P*-value < 0.05).
78 Grey dots are not differentially expressed. Multiple CPA genes are labeled.
79
80

Supplemental Fig S7

A

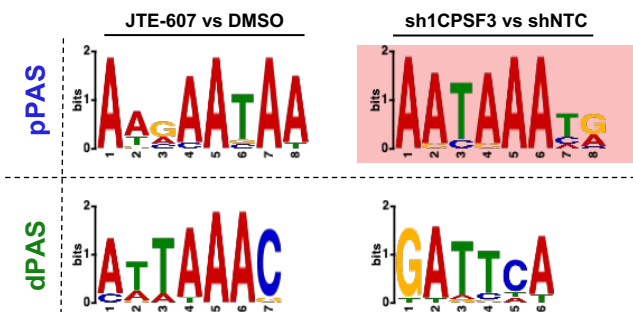


B



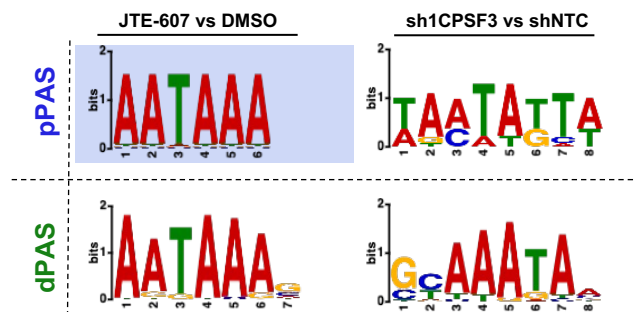
C

Unique 3'UTR shortening genes



D

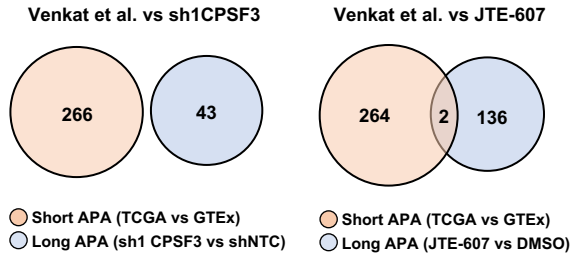
Unique 3'UTR lengthening genes



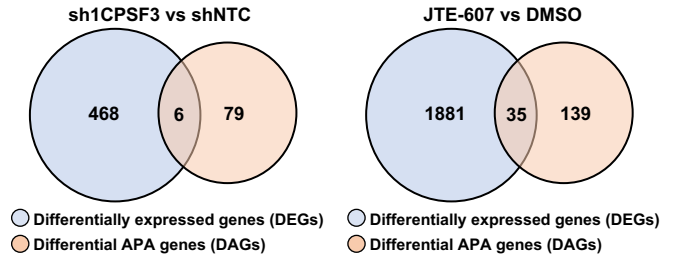
81 **Fig. S7. PAS surrounding motifs of DAGs are distinct between knockdown and**
82 **inhibition.**
83 **(A, B)** The distribution of the NUDT21 binding motif, UGUA, surrounding PASs of genes
84 undergoing shortening events upon *CPSF3* knockdown (A) and inhibition (B). Green
85 and blue lines represent the distribution of UGUA around the proximal and distal PAS,
86 respectively. **(C, D)** Motif enrichment analyses of Top sequences surrounding PASs of
87 APA short **(C)** and long **(D)** genes upon *CPSF3* inhibition (left) and knockdown (right).
88
89

Supplemental Fig S8

A



B

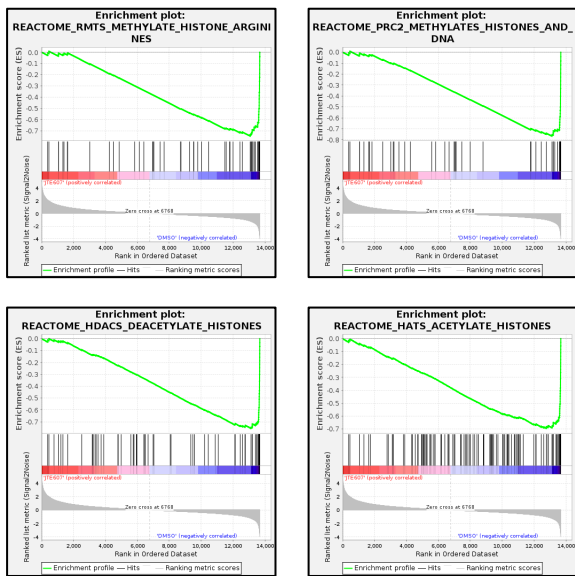


90 **Fig. S8. Clinically APA altered genes are not affected by CPSF3 disruption.**
91 **(A)** Venn diagrams of short APA genes from TCGA-PAAD (Venkat et al.) data and Long
92 APA genes upon *CPSF3* knockdown and inhibition, respectively. **(B)** Venn diagrams of
93 differential APA genes (DAGs) and differentially expressed genes (DEGs) upon *CPSF3*
94 knockdown and inhibition, respectively.

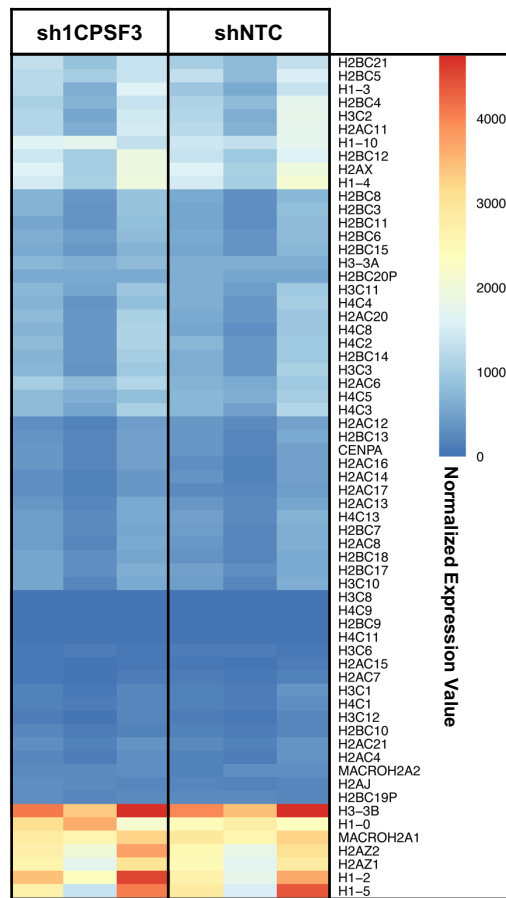
95
96

Supplemental Fig S9

A



B



C

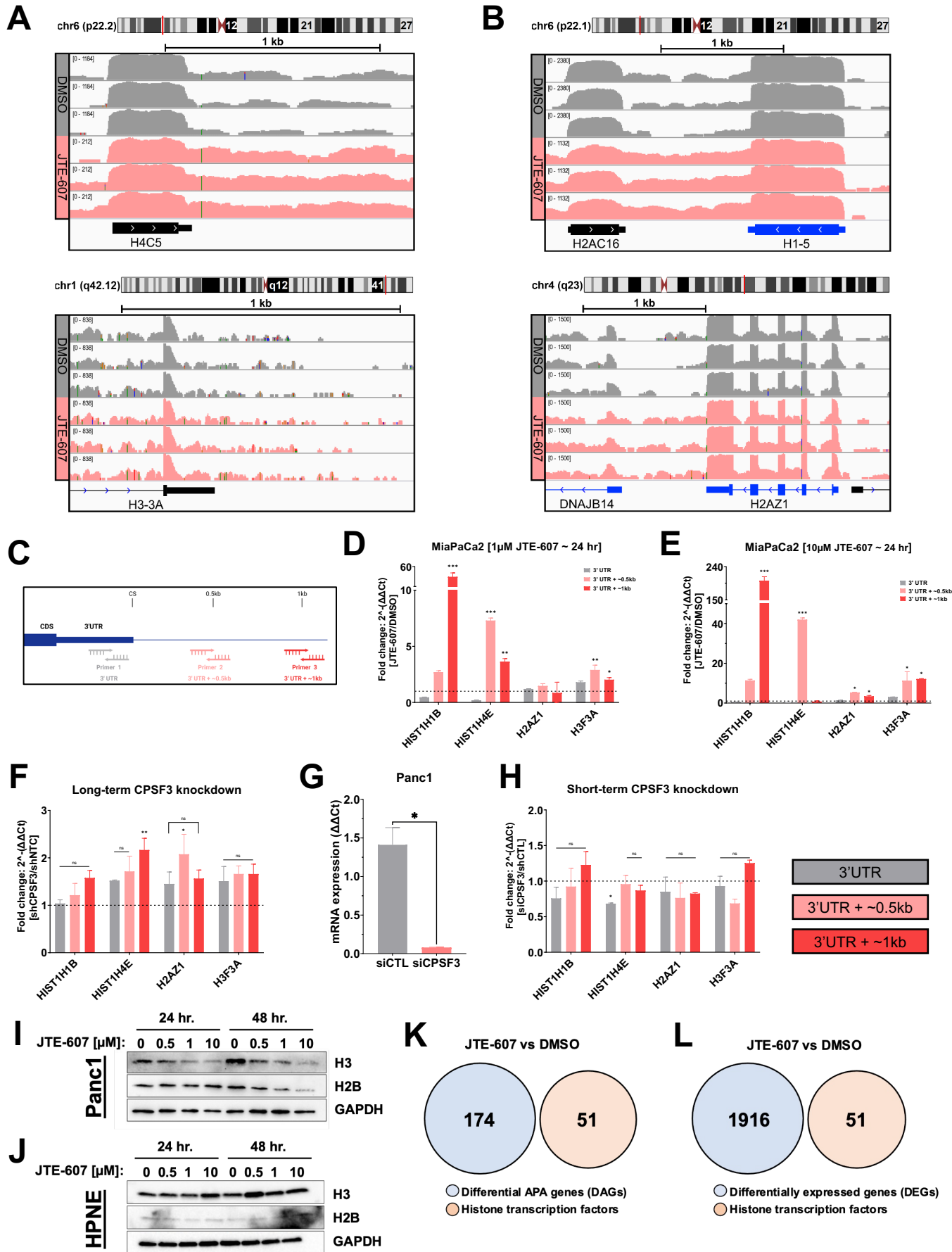
Differentially expressed genes



- JTE-607 vs DMSO
- sh1 CPSF3 vs shNTC

97 **Fig. S9. Replication-dependent histones are not affected by *CPSF3* knockdown.**
98 **(A)** Gene set enrichment analysis (GSEA) from RNA-seq data upon 10 μ M JTE-607
99 treatment. **(B)** Heatmap of normalized expression values from DESeq2 results in Panc1
100 cells upon *CPSF3* knockdown. Expression is plotted as normalized expression values.
101 **(C)** Venn diagrams of differentially expressed genes upon *CPSF3* knockdown (orange)
102 and inhibition (blue). Only 119 genes are differentially expressed in both conditions.
103
104
105

Supplemental Fig S10

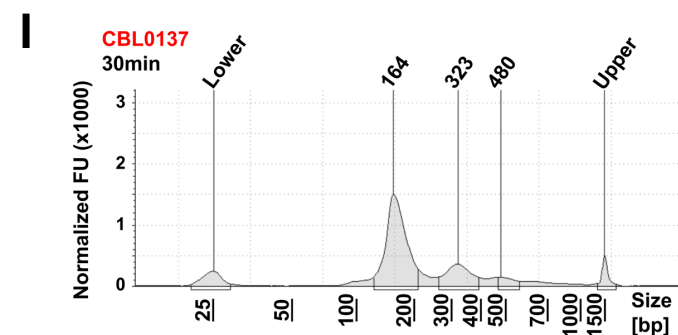
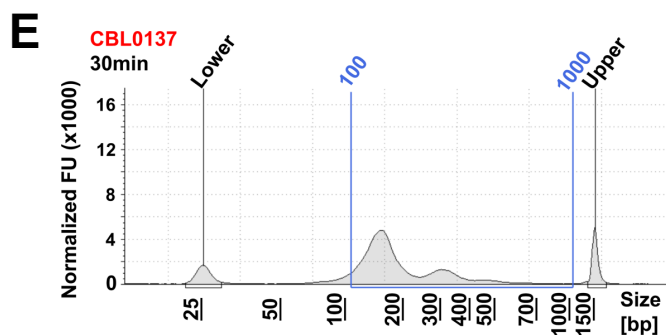
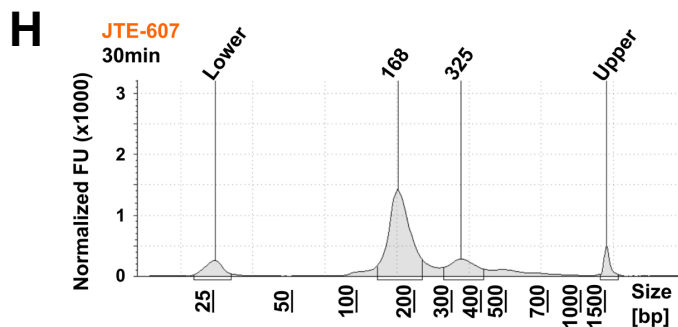
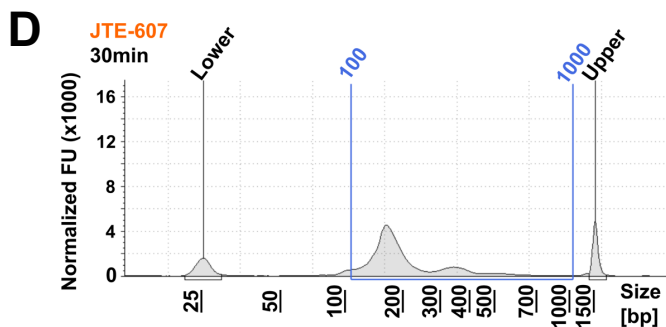
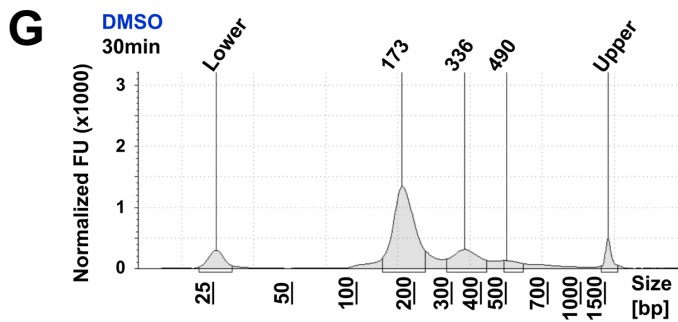
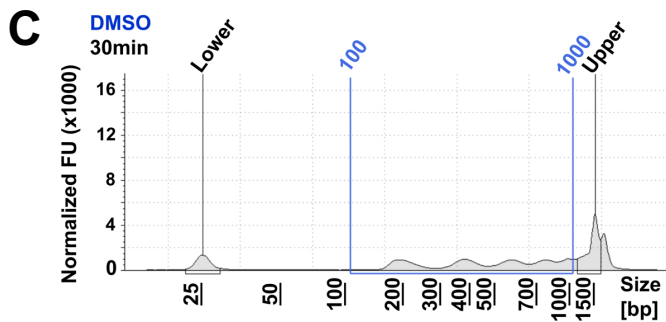
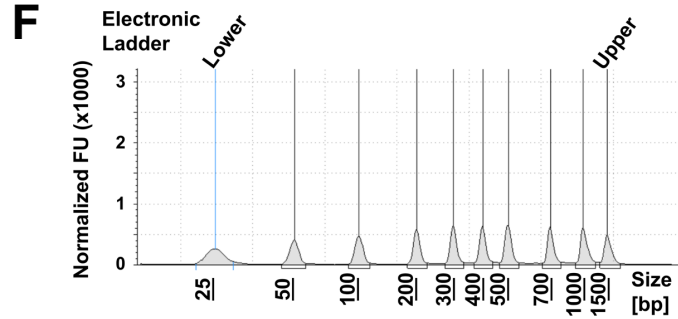
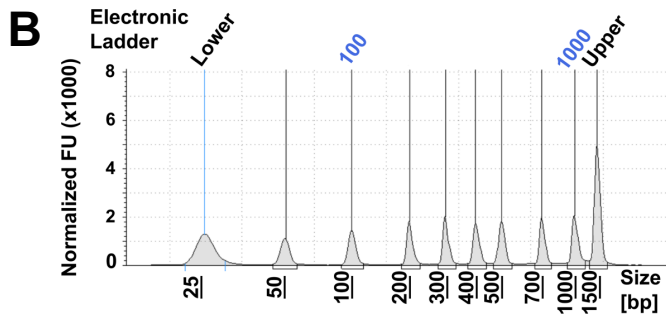


106 **Fig. S10. JTE-607 induces transcriptional read-through in RD histones.**
107 **(A)** UCSC genome browser-generated density plots of two representative replication-
108 dependent histones highlighting the differences of read coverage beyond the 3'UTR
109 boundaries upon 24hr of JTE-607 treatment (pink) relative to DMSO control group (grey)
110 using total RNA-seq data. **(B)** UCSC genome browser-generated density plots of two
111 representative replication-independent histones highlighting the differences of read
112 coverage beyond the 3'UTR boundaries upon 24hr of JTE-607 treatment (pink) relative
113 to DMSO control group (grey) using total RNA-seq data. Y-axes indicates Log(read
114 density). **(C)** Schematic showing primer design for read-through quantification by RT-
115 qPCR. **(D, E)** Quantification of replication-dependent histone read-through in MiaPaCa2
116 cells after 24 hr of **(D)** 1 μ M and **(E)** 10 μ M of JTE-607 treatment by RT-qPCR. Data were
117 normalized to DMSO controls (Dashed horizontal line). *, $P < 0.05$; **, $P < 0.01$; ***, $P <$
118 0.001; 2-way ANOVA with Sidak's multiple comparisons test. **(F)** Quantification of histone
119 read-through in Panc1 upon long-term *CPSF3* knockdown by shRNA by RT-qPCR. **(G)**
120 Quantitative RT-qPCR showing *CPSF3* mRNA expression levels in Panc1 cells upon
121 *CPSF3* transient knockdown by siRNA. Data are shown as mean \pm SEM. *, $P < 0.05$,
122 unpaired t test. **(H)** Quantification of histone read-through in Panc1 upon short-term
123 *CPSF3* knockdown using siRNA by RT-qPCR. Data were normalized to non-targeting
124 controls (Dashed horizontal line). *, $P < 0.05$; **, $P < 0.01$; 2way ANOVA with Sidak's
125 multiple comparisons test. **(I, J)** Protein levels of H3 and H2B histones upon JTE-607
126 treatment in Panc1 (I) and HPNE (J) cells. **(K, L)** Venn diagrams showing the overlap
127 between histone transcription factors and significant APA-altered genes (DAGs) **(K)**
128 or differentially expressed genes (DEGs) **(L)** upon JTE-607 treatment.
129
130

Supplemental Fig S11

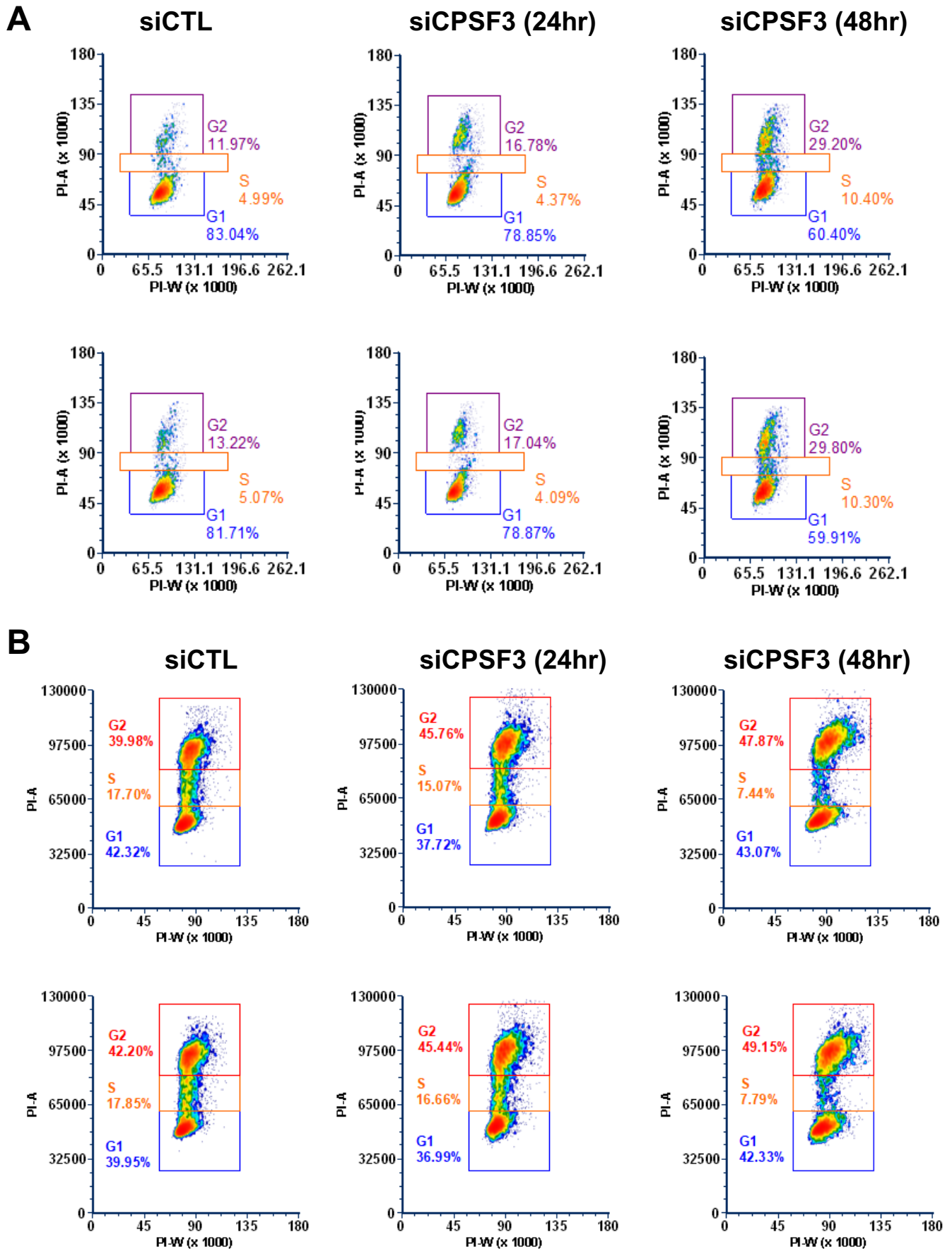
A

Term	P-value	FDR	Combined Score
Chromatin assembly (GO:0031497)	7.36E-06	0.006693444	130.922877
Nucleosome assembly (GO:0006334)	2.17E-05	0.00884124	128.7851932
Mitochondrial cytochrome c oxidase assembly (GO:0033617)	3.83E-05	0.00884124	262.0222728
Nucleosome organization (GO:0034728)	3.89E-05	0.00884124	85.24289775
Establishment of protein localization to chromatin (GO:0071169)	5.01E-05	0.009110558	609.5011178



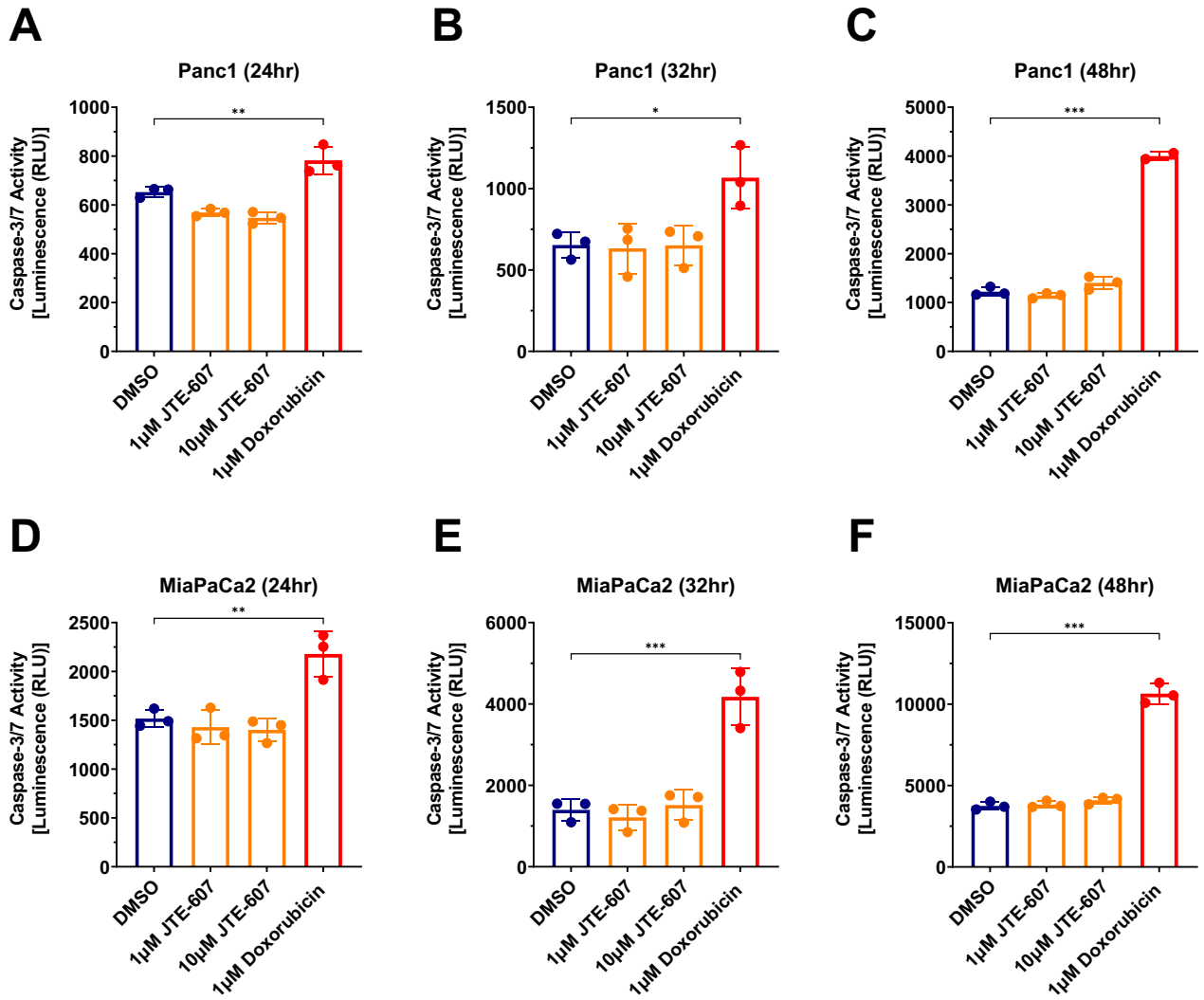
131 **Fig. S11. JTE-607 increases genomic DNA digestion in Panc1 cells.**
132 **(A)** Gene ontology analysis of significantly downregulated genes upon JTE-607
133 treatment. Enrichr was used to perform the analysis. **(B - E)** Nucleosome intensity plots
134 of Panc1 cells upon 10 μ M JTE-607 treatment for 24 hr. Reference ladder shown in **(B)**.
135 Lower base pair sizes indicate more digestion at that specific size. The intensity of
136 digestion is represented by the Y-axis. **(F - I)** Nucleosome intensity plots of HPNE cells
137 upon 10 μ M JTE-607 treatment for 24 hr. Reference ladder shown in **(F)**. Lower base pair
138 sizes indicate more digestion at that specific size. The intensity of digestion is represented
139 by the Y-axis.
140
141

Supplemental Fig S12



142 **Fig. S12. S-phase population upon CPSF3 knockdown.**
143 **(A-B)** Quantification of cells in the S-phase upon transient knockdown of CPSF3 by
144 siRNA in HPNE cells **(A)** and Panc1 cells **(B)** after 24hr (middle panels) and 48hr (right
145 panels) as compared to non-targeting controls (siCTL, left panels).
146
147

Supplemental Fig S13



148 **Fig. S13. JTE-607 does not induce significant levels of apoptosis in PDAC cells.**
149 **(A-F)** Caspases 3/7 activity upon 1 μ M (yellow bars) and 10 μ M of JTE-607 treatment as
150 compared to 0.1% DMSO (blue bars) and 1 μ M Doxorubicin as a positive control (red
151 bars) for 24hr **(A and D)**, 32hr **(B and E)** and 48hr **(C and F)** in Panc1 (top panels) and
152 MiaPaCa2 (bottom panels) cells. *, $P < 0.05$; **, $P < 0.01$; ***, $P < 0.001$; Ordinary one-
153 way ANOVA with Dunnett's multiple comparisons test.

154
155

156 **Materials and Methods**

157 **Cell lines and *in vitro* culture**

158 HEK293T, MiaPaCa2, Panc1, Suit2, Human immortalized C7 CAFs and PancPat CAFs
159 cells were cultured in DMEM (DMEM [+] 4.5 g/L glucose, L-glutamine, sodium pyruvate)
160 supplemented with 10% fetal bovine serum (FBS) and 1% penicillin-streptomycin. Non-
161 transformed pancreatic cell line HPNE cells were cultured in 75% DMEM+25% Medium
162 M3 Base supplemented with 2mM L-glut, 1.5g/L sodium bicarbonate, 5% FBS, 10ng/mL
163 hEGF and 5.5mM D-glucose. Non-transformed pancreatic cell line HPDE cells were
164 cultured in Keratinocyte SFM (serum-free media) supplemented with 25mg BPE, 2.5µg
165 EGF, 1X anti-anti and 50µg/mL Gentamicin. HeLa-TI cells were cultured in phenol red-
166 free FluoroBrite DMEM complete Media. All cell lines were cultured at 37°C with 5% CO₂
167 and tested negative for Mycoplasma.

168

169 **Generation of stable and transient CPSF3 knockdown cells**

170 For stable knockdown, two vectors expressing short-hairpin RNA (shRNA) targeting
171 CPSF3 were purchased from Sigma-Aldrich. Cells were infected with lentivirus harboring
172 pLKO.1-shNTC (non-targeting control) and pLKO.1-shCPSF3 at 40% confluency.
173 Polybrene was used to increase the efficacy of infection. After 72 hours, cells were
174 selected with 2.5µg/ml puromycin. Knockdown was confirmed by qPCR and
175 immunoblotting. For transient knockdown, cells were plated at $\sim 1.5 \times 10^5 - 2.5 \times 10^5$ cells
176 per well in a 6-well plate one day prior to transfection. The next day cells were transfected
177 with 60nM of siRNA against CPSF3 and a non-targeting control. Transfection media were
178 replaced with complete media 6h after transfection. After 24h and 48h of transfection,
179 cells were collected for subsequent experiments.

180

181 **RNA isolation and quantitative PCR**

182 Cells were lysed with TRIzol reagent. RNA was isolated using Direct-zol RNA Miniprep.
183 cDNA was synthesized using iScript cDNA Synthesis Kit. qPCR was conducted with
184 SYBR Green pre-designed PCR primers (IDT or Bio-Rad) mixed with iTaq Universal
185 SYBR Green Supermix and run on CFX connect systems (Bio-Rad). For read-through

186 qPCR quantification, primers were designed and ordered from IDT and are listed in Table
187 S1. Data were analyzed in Microsoft Excel and graphed using GraphPad Prism (v 9.3.0).

188

189 **RNA-sequencing**

190 For each condition, three biological samples were sequenced. All the sequencing was
191 done on total RNA (ribosomal RNA depleted) and primed with random primers. Briefly,
192 cells were trypsinized, washed with 1X PBS and sent frozen (-80°C) for RNA sequencing
193 (RNA-seq). 500ng total RNA was used to prepare the sequencing libraries using KAPA
194 RNA HyperPrep Kit with RiboErase (HMR) (Roche Sequencing Solutions) following
195 manufacturer's protocol. Briefly, ribosomal RNA (rRNA) was depleted from total RNA and
196 DNase-digested to remove gDNA contamination. RNA was purified, fragmented and first
197 strand cDNA was synthesized using random primers. cDNA:RNA hybrids were converted
198 into double-stranded cDNA (dscDNA) using dUTP incorporation. Adapters were added to
199 the 3' ends, ligated to library insert fragments and the library amplified in a strand-specific
200 manner. Data were analyzed by the Bioinformatics Shared Resource (Roswell Park
201 Comprehensive Cancer Center).

202

203 **Nuclear isolation**

204 Cells were grown and collected at 80-90% confluence for nuclei isolation. Briefly, Cells
205 were washed with cold 1X PBS and then incubated with hypotonic buffer (10mM Tris pH
206 8, 1.5mM MgCl₂, 2mM KCl) for 15 minutes. Cells were scraped and nuclei release was
207 assessed under the microscope using trypan blue staining. Cell suspension was
208 centrifuged at 2000 rpm for 5 minutes at 4°C. Pellets were washed with hypotonic buffer
209 and centrifuged at 700 x g for 5 minutes at 4°C. Pellets (nuclei) were lysed using NP40
210 lysis buffer for 1 hour while rotating at 4°C and sonicated once at the end. Nuclear lysate
211 was centrifuged at max speed for 10 minutes at 4°C. Supernatant was collected as the
212 final nuclear lysate.

213

214 **Immunoprecipitation**

215 Immunoprecipitation was performed using protein G beads. Briefly, beads were mixed
216 thoroughly and washed twice with 1X TBS-T buffer (25mM Tris, 0.15M NaCl, 0.05%

217 Tween-20 Detergent) containing protease and phosphatase inhibitors. Beads were
218 collected using magnetic stand to remove wash buffer. To preclear the samples, 1 mg of
219 sample was added to the beads and incubated with rotation for 1 hour at 4°C. Beads were
220 separated from the lysate using magnetic stand, and precleared samples were
221 transferred to a clean tube. New magnetic beads (~25ul/1ml lysate) were washed twice,
222 and precleared samples were added to the beads. Antibodies (IgG control or target
223 antibody) were added to lysates and incubated overnight on rotator at 4°C. Beads were
224 collected using magnetic stand and supernatant (unbound proteins) was discarded.
225 Magnetic beads were washed twice with cold 1X TBS-T buffer and once with ultrapure
226 water then collected on magnetic stand. Finally, beads were incubated with 100ul of SDS-
227 PAGE Sample Buffer containing reducing agent at 95°C for 5-10 minutes. Magnetic beads
228 were separated, and the supernatant was used for western blot analysis.

229

230 **Immunoblotting**

231 For whole cell lysates, samples were lysed using RIPA lysis buffer (50mM Tris. HCl pH
232 7.5, 150mM NaCl, 5mM EDTA pH 8, 1% Triton X-100, 0.5% NP-40) in the presence of
233 10ug/ml protease inhibitors (Aprotinin, Leupeptin, PMSF), boiled at 95°C for 5min and
234 resolved by SDS-PAGE. Proteins were transferred to nitrocellulose membranes at a
235 constant voltage of 100V for 70 minutes at 4°C using Mini Trans-Blot® Cell (Bio-Rad).
236 Membranes were blocked in TBST (Tris-buffered saline (TBS) with 0.1% v/v TWEEN-20)
237 and 5% w/v nonfat dry milk. Primary antibodies (listed in Table S2) were diluted in 3%
238 BSA in TBST and incubated overnight at 4°C. Membranes were incubated with
239 horseradish peroxidase-conjugated secondary antibodies at 1:2,000 for 1 hour at room
240 temperature. Pierce ECL Western Blotting Substrate or Supersignal West Femto
241 Maximum Sensitivity substrate were used for chemiluminescent detection. Signals were
242 visualized and imaged using the ChemiDoc XRS+ System and Image Lab Software (Bio-
243 Rad).

244

245 **Proliferation and clonogenicity assays**

246 For proliferation experiments, cells were seeded at a density of 250 cells/well (MiaPaCa2
247 and Panc1 cells) or 1000 cells/well (HPNE cells) into a white 96-well plate in triplicate.

248 Cell proliferation was measured using CellTiter-Glo Luminescent Cell Viability Assay Kit
249 at days 0, 2, 4 and 6. For clonogenicity assays, cells were seeded at a density of 500
250 cells/well into a 6-well plate in triplicate. After 11 days, cells were fixed with 4% formalin,
251 stained with 0.2% Crystal Violet and images were obtained for analysis. Colony area was
252 measured using ImageJ software. Data were normalized to control data points.

253

254 **Caspase 3/7 activity assay**

255 Panc1 and MiaPaCa2 cells were seeded at a density of 1000 cells per well in 384-well
256 plate. Cells were then treated with 1 μ M and 10 μ M of JTE-607 as well as 1 μ M of
257 Doxorubicin as a positive control. Caspase3/7 activity were then detected by measuring
258 luminescence using the Caspase-Glo® 3/7 Assay System (Promega; Cat# G8091).

259

260 **Cell cycle analysis**

261 Cells were trypsinized and resuspended in 1X PBS, then fixed with ice-cold 70% ethanol
262 for 1 hour at -20°C. Cells were then washed with cold 1X PBS and incubated with RNaseA
263 (200 μ g/ml) at 37°C for 1 hour. Propidium iodide (40 μ g/ml) was then added, incubated for
264 1 hour in the dark and analyzed by FACS at 488nm. Data were analyzed by FCS express
265 software (v7.06.0015).

266

267 **BrdU incorporation assay**

268 Cells were cultured under optimum conditions and incubated with 50 μ M BrdU (5-Bromo-
269 2'-deoxyuridine; Sigma-Aldrich; B5002) for 4 hours. Cells were then rinsed with 1X PBS,
270 trypsinized, permeabilized in 70% ice cold ethanol with gentle vortexing and stored at -
271 20°C overnight. Next, cells were pelleted and DNA was hydrolyzed by incubating with
272 500 μ l of 2N HCl, 0.5% Triton X-100 in 1X PBS, incubated for 30 minutes at room
273 temperature and then neutralized by adding 1.5ml of 0.1 M sodium tetraborate (pH 8.5)
274 for 2 minutes. Cells were then pelleted, washed once with 1% BSA in 1X PBS and
275 resuspended in 50 μ l 0.5% Tween 20, 1% BSA in 1X PBS. Next, 10⁶ cells were incubated
276 with 1 μ g Anti-BrdU-FITC for 1 hour at room temperature. Cell pellets were washed once
277 with 150 μ l 1% BSA in 1X PBS, resuspended in 500 μ L 1X PBS with RNaseA (200 μ g/ml)
278 and PI (40 μ g/ml) and incubated at room temperature for 30 minutes in the dark. Cells

279 were analyzed by flow cytometry immediately and a compensation step was performed.
280 Data were analyzed by FCS Express software (v7.06.0015).

281

282 **Xenograft experiments**

283 Animal experiments were approved by the Roswell Park Institutional Animal Care and
284 Use Committee. MiaPaCa2 cells infected with shNTC and sh1 CPSF3 constructs were
285 trypsinized, washed with 1X PBS and counted. 5×10^5 cells were resuspended in 50 μ l of
286 1X PBS/Matrigel in a 1:1 ratio and injected subcutaneously into the flanks of 8-week old
287 NOD/SCID/IL2R $\gamma^{-/-}$ (NSG) mice. When palpable, tumor volume was determined by caliper
288 measurements obtained in 2 dimensions and calculated as $\text{width}^2 \times \text{length}/2$ twice a
289 week. Mice were euthanized when the first tumor reached 1400 mm^3 , tumors were
290 dissected, and tumor volumes were measured.

291

292 **Histology and Immunohistochemistry**

293 Freshly dissected tumors were fixed in 10% neutral buffered formalin solution (Sigma-
294 Aldrich, Cat. # HT501128) for 24 hours prior to processing. Tumor processing was
295 performed by the Experimental Tumor Model (ETM) Shared Resource team at RPCC.
296 Briefly, Formalin-fixed paraffin embedded (FFPE) blocks were sectioned (5 μ m),
297 rehydrated, stained with hematoxylin and eosin, dehydrated, dried, and mounted. For
298 immunohistochemistry, after deparaffinization and rehydration, antigen unmasking was
299 performed using Retriever 2100 pressure cooker (Aptum). Slides were then
300 immunostained overnight at 4°C, washed, treated with ImmPRESS Polymer reagent
301 (Vector Laboratories) and counterstained. Slides were visualized using OLYMPUS BX41
302 microscope, imaged using CellSens Standard software and analyzed using ImageJ.

303

304 **JTE-607 studies**

305 For dose-response measurements, cells were seeded at a density of 1000 cells per well
306 in a 96-well white plate. The next day, JTE-607 was titrated over a range of concentrations
307 using the Tecan D300e Digital Dispenser and cell viability was measured 72 hours post
308 drug titration using a CellTiter-Glo Luminescent Cell Viability Assay Kit (Promega). For
309 cell proliferation experiments, cells were seeded at a density of 250 cells per well in a 96-

310 well white plate. DMSO control or JTE-607 was dispensed at varying concentrations and
311 proliferation was measured using CellTiter-Glo Assay at days 0, 2, 4 and 6. For
312 clonogenicity experiments, cells were seeded at a concentration of 500 cells per well and
313 treated with different concentrations of JTE-607. Cells were allowed to grow over a period
314 of 11-14 days after which they were fixed in 10% formalin, stained with 0.2% Crystal Violet
315 and images were obtained for analysis. Colony area was measured using ImageJ
316 software. Data were normalized to DMSO control data points.

317

318 **Micrococcal digestion**

319 Micrococcal Nuclease (MNase) was performed as previously described (Safina et al.
320 2017). Briefly, cells were trypsinized, washed with 1X RSB buffer (10mM Tris HCL, pH7.6;
321 15mM NaCl; 1.5mM MgCl₂) and pelleted at 1000rpm for 4 minutes at room temperature.
322 Cell pellets were resuspended in 1X RSB buffer with 1% TritonX-100, homogenized with
323 a loose pestle (5 strokes) and centrifuged for 5 minutes at 2000rpm at 4°C. Pellets were
324 washed two times with 1ml of buffer A (10mM Tris HCL, pH7.6; 15mM NaCl; 60mM KCl;
325 0.34M Sucrose; 0.1% B-mercaptoethanol; 0.15mM Spermine; 0.5 mM Spermidine;
326 0.25mM PMSF) and nuclei were pelleted at 160g for 10 minutes at 4°C. Nuclei were
327 resuspended in 1.5ml of buffer A supplemented with 1mM of CaCl₂. Nuclear suspensions
328 (500µl) were digested with 200U/ml Micrococcal nuclease at 37°C at different time points.
329 Digestion was inactivated by 15mM EDTA. 10%SDS and 1M NaCl were added to extract
330 genomic DNA. DNA was run and visualized using TapeStation 4200 system.

331

332 **Bioinformatics Analyses**

333 **Differential gene expression analysis**

334 Raw sequencing reads passed quality filter from Illumina RTA were first pre-processed
335 by using FASTQC (v0.11.8) for sequencing base quality control. The reads were mapped
336 to GRCh38 human reference genome and GENCODE (v38) (Kent et al. 2002) annotation
337 database using STAR (v2.7.9a) (Dobin et al. 2013). Alignment files are indexed using
338 samtools (v1.14) (Li et al. 2009). A Second pass QC was done using alignment output
339 with RSeQC (v4.0.0) (Wang et al. 2012) to examine abundances of genomic features,
340 splicing junction saturation and gene-body coverage. Gene expression was quantified

341 using featureCounts (v2.0.0) (Liao et al. 2014) with --fracOverlap 1 option and then
342 formatted in a raw counts data matrix. Differential expression analyses were performed
343 with DESeq2 (v1.36.0) (Love et al. 2014), a variance-analysis package developed to infer
344 statistically significant differences in RNA-seq data using a Negative Binomial GLM.
345 Genes are called differentially expressed (DE) when having a Fold-Change (FC) > 1.5
346 and FDR < 0.05 (using Benjamini-Hochberg method to control false discovery rate).
347 Downstream and visualization plots were done using regularized-log2 transformation
348 implemented by DESeq2. Heatmaps were generated using the pheatmap (v1.0.8) R
349 package.

350

351 **3'UTR alternative polyadenylation analysis**

352 For each sample, PCR duplicates were identified using UMI bar codes. UMI tools extract
353 was used to extract the UMI nucleotides from the reads and append them to the read
354 names. Initial quality control was performed using fastp. Reference human genome and
355 annotations of the build GRCh38 release 33 were downloaded from the GENCODE
356 portal. UMI marked and trimmed reads were aligned to respective reference genomes
357 using STAR version 2.7.3a (Dobin et al. 2013). Sample-wise alignments were saved as
358 Sequence Alignment Map (SAM) files. SAMtools V0.1.19 'view', 'sort' and 'index' modules
359 were used to convert the SAM files to Binary Alignment Maps (BAM) files, sort by
360 chromosomal coordinates, and index respectively (Danecek et al. 2021). Mapped reads
361 are deduplicated using UMI tools dedup based on the UMI marked read names and the
362 mapping coordinates (Smith et al. 2017). Alternative polyadenylation (APA) analysis was
363 performed using PolyAMiner-Bulk. Samples were processed with the following
364 parameters: -a 0.65 -pa_p 1 -pa_a 5 -pa_m 5 -outPrefix 3UTROnly -expNovel 1 -s 2 -
365 ignore UTR5,CDS,Intron,UN -apriori_annotations -modelOrganism human. APA analysis
366 focusing only on 3'UTR regions was performed by excluding the polyA sites mapped to
367 other genomic regions with the parameter -ignore UTR5,CDS,Intron,UN. Total reads per
368 feature were computed by adding all individual C/PAS site counts mapped to respective
369 features and total gene counts were computed as the sum of all individual feature C/PAS
370 counts. A beta-binomial test was performed using the proportions of individual feature
371 counts to the total gene counts to infer differential C/PAS usage changes. Our RNA-seq

372 was based on random priming which does not specifically enrich for polyadenylated RNAs
373 as oligo(dT) priming would. PolyAMiner-Bulk overcomes the challenges associated with
374 identifying polyadenylation sites in random priming-based RNA-seq. PolyAMiner-Bulk is
375 adept at inferring changes in alternative polyadenylation (APA) from bulk RNA-Seq
376 datasets. It enhances the detection process by integrating both established reference
377 polyadenylation sites and newly detected Cleavage and Polyadenylation Sites (C/PASs).
378 It further refines the candidate C/PASs by applying a deep learning model called C/PAS-
379 BERT and utilizing vector projections to analyze alternative polyadenylation (APA)
380 patterns within genes. It is important to note that PolyAMiner-Bulk does not solely rely on
381 RNA primed with oligo-dT (also known as softclipped reads) to pinpoint alternative
382 polyadenylation sites (C/PASs). While some existing tools in this field depend exclusively
383 on softclipped reads to identify candidate C/PASs for subsequent APA analysis, our
384 approach is more comprehensive. PolyAMiner-Bulk combines both established reference
385 C/PASs from databases like PolyASite and PolyADB with newly identified C/PASs to
386 create a larger candidate C/PAS library and retain only high-confidence C/PASs from our
387 candidate library. This approach offers several advantages. It allows us to leverage
388 existing C/PAS annotations and sequencing biochemistry to (i) detect a greater number
389 of C/PASs, (ii) distinguish C/PASs that are closely located, and (iii) overcome sensitivity
390 limitations associated with relying solely on softclipped or oligo (dT) reads.

391

392 **Motif enrichment analysis**

393 To discover novel, ungapped motifs of recurring, fixed-length patterns in our sequence
394 datasets, we employed the STREME methodology (Bailey et al. 2015). STREME (Simple,
395 Thorough, Rapid, Enriched Motif Elicitation) discovers ungapped motifs that are enriched
396 in our sequence datasets. The enriched motifs were derived by first identifying unique
397 3'UTR shortened and lengthened genes for both the *CPSF3* knockdown and JTE-607
398 conditions. Subsequently, we extracted sequences that are 100 nucleotides in length,
399 flanking the 50 base pairs upstream and downstream of the most proximal and distal
400 cleavage sites, referencing the sequence database Human hg38
401 (UCSCMammal/hg38.fna). Consequently, we obtained four distinct sets of sequences: a
402 pair of proximal and distal sequences for both the *CPSF3* knockdown and JTE-607

403 conditions. Lastly, we used the STREME program to find enriched motifs. The program
404 shuffles each set to create a corresponding control set and uses a Fisher's Exact Test to
405 determine significance of each motif found in the positive set as compared with its
406 representation in the control set, using an adjusted p-value significance threshold of 0.05.
407 Only significant motifs were shown in the figures.

408

409

410 **Quantification and Statistical Analysis**

411 **Image analysis**

412 Raw images were obtained and processed using ImageJ, CellSens Standard and Image
413 Lab software.

414

415 **Statistical analyses**

416 Experimental findings were obtained from at least two independent experiments.
417 Statistics were performed in GraphPad Prism 9. In general, $P < 0.05$ was considered
418 statistically significant. All statistical methods and P-values are provided in the figure
419 legends. Asterisks in graphs denote statistically significant differences as described in
420 figure legends.

421

Table S1. Primer pairs used to quantify histone read-through by RT-qPCR.

Target	Primer pair	Primer direction	5' – 3' sequence
<i>H1-5</i> (<i>HIST1H1B</i>)	3'UTR (P1)	Forward primer	TGTTGCGGTTTTCACACGC
		Reverse primer	CTAAAGCTGCAAAGGCCAAGAA
	3'UTR+~0.5kb (P2)	Forward primer	AGACCCCATCTTGAAACTTGC
		Reverse primer	AGCCATTTAGGCACCAGCTA
	3'UTR+~1kb (P3)	Forward primer	AGAGCTGGGCCACTGGTTA
		Reverse primer	TTCCTAAAAGTCATTCCTAAGCTCT
<i>H4C5</i> (<i>HIST1H4E</i>)	3'UTR (P1)	Forward primer	ACAGGGACGCACTCTTTACG
		Reverse primer	TGGGAAGTCGAGATGCTGAG
	3'UTR+~0.5kb (P2)	Forward primer	GCTCACGCAAGGAGAGGTT
		Reverse primer	ACTTCTAAGGGACAACCTGGGT
	3'UTR+~1kb (P3)	Forward primer	TCCACAGTTATGCCCCAGATG
		Reverse primer	CACAACGGAAGTTATGGCTGG
<i>H2AFZ</i> (<i>H2AZ1</i>)	3'UTR (P1)	Forward primer	ACTGGAATCACCAACACTGGA
		Reverse primer	ACTGTCTAAAGGATGCCTGGA
	3'UTR+~0.5kb (P2)	Forward primer	ATTCACCTTTTCCGTCCCA
		Reverse primer	CCGCGAAGACTAACAAGACAC
	3'UTR+~1kb (P3)	Forward primer	GAAGGGGACACTCGTTTTCA
		Reverse primer	CGCATCCTCCCTCGCTTG
<i>H3F3A</i> (<i>H3-3A</i>)	3'UTR (P1)	Forward primer	AGAATCCACTATGATGGGAAACA
		Reverse primer	TCCCCTATTTTTCCACTCGC
	3'UTR+~0.5kb (P2)	Forward primer	AACTGCCCTAGAAGTGATACGA
		Reverse primer	GCAGTAAGAATGCAAGCCCA
	3'UTR+~1kb (P3)	Forward primer	ACTATGTGCTCACTGTCCAGGT
		Reverse primer	GTACATACGTTGAGTGCCAAGT

424

Table S2. Primary antibodies list.

Primary antibody target	Application	Vendor	Antibody ID
GAPDH	WB	Proteintech	60004-1-Ig
CPSF2	IP & WB	Novus Biologicals	NB100-79823
CPSF3	WB	Abcepta	AT1610a
CPSF3	IHC	Atlas Antibodies	HPA034657
CPSF4	IP & WB	Novus Biologicals	NB100-79826
NUDT21	IP & WB	Santa Cruz	sc-81109
CFIm68	IP & WB	Bethyl Laboratories	A301-358A
CSTF2	IP & WB	Bethyl Laboratories	A301-092A
CSTF3	IP & WB	Santa Cruz	SC-376575
FITC anti-BrdU	FACS	BioLegend	364104
Ki67	IHC	Novus Biologicals	NB600-1209

425

426 **References**

- 427 Bailey TL, Johnson J, Grant CE, Noble WS. 2015. The MEME Suite. *Nucleic Acids Res*
428 **43**: W39-49.
- 429 Danecek P, Bonfield JK, Liddle J, Marshall J, Ohan V, Pollard MO, Whitwham A, Keane
430 T, McCarthy SA, Davies RM, et al. 2021. Twelve years of SAMtools and BCFtools.
431 *Gigascience* **10**: giab008. <https://doi.org/10.1093/gigascience/giab008>.
- 432 Dobin A, Davis CA, Schlesinger F, Drenkow J, Zaleski C, Jha S, Batut P, Chaisson M,
433 Gingeras TR. 2013. STAR: ultrafast universal RNA-seq aligner. *Bioinformatics* **29**:
434 15–21. <https://doi.org/10.1093/bioinformatics/bts635>.
- 435 Kent WJ, Sugnet CW, Furey TS, Roskin KM, Pringle TH, Zahler AM, Haussler D. 2002.
436 The human genome browser at UCSC. *Genome Res* **12**: 996–1006.
- 437 Li H, Handsaker B, Wysoker A, Fennell T, Ruan J, Homer N, Marth G, Abecasis G,
438 Durbin R. 2009. The Sequence Alignment/Map format and SAMtools.
439 *Bioinformatics* **25**: 2078–2079.
- 440 Liao Y, Smyth GK, Shi W. 2014. featureCounts: an efficient general purpose program
441 for assigning sequence reads to genomic features. *Bioinformatics* **30**: 923–930.
- 442 Love MI, Huber W, Anders S. 2014. Moderated estimation of fold change and
443 dispersion for RNA-seq data with DESeq2. *Genome Biol* **15**: 1–21.
- 444 Safina A, Cheney P, Pal M, Brodsky L, Ivanov A, Kirsanov K, Lesovaya E, Naberezhnov
445 D, Neshher E, Koman I, et al. 2017. FACT is a sensor of DNA torsional stress in
446 eukaryotic cells. *Nucleic Acids Res* **45**: 1925–1945.
- 447 Smith T, Heger A, Sudbery I. 2017. UMI-tools: Modeling sequencing errors in Unique
448 Molecular Identifiers to improve quantification accuracy. *Genome Res* **27**: 491–499.
- 449 Wang L, Wang S, Li W. 2012. RSeQC: quality control of RNA-seq experiments.
450 *Bioinformatics* **28**: 2184–2185.
451